RSC Advances

Accepted Manuscript

This is an *Accepted Manuscript*, which has been through the RSC Publishing peer review process and has been accepted for publication.

Accepted Manuscripts are published online shortly after acceptance, which is prior to technical editing, formatting and proof reading. This free service from RSC Publishing allows authors to make their results available to the community, in citable form, before publication of the edited article. This *Accepted Manuscript* will be replaced by the edited and formatted *Advance Article* as soon as this is available.

To cite this manuscript please use its permanent Digital Object Identifier (DOI®), which is identical for all formats of publication.

More information about *Accepted Manuscripts* can be found in the **Information for Authors**.

Please note that technical editing may introduce minor changes to the text and/or graphics contained in the manuscript submitted by the author(s) which may alter content, and that the standard **Terms & Conditions** and the **ethical guidelines** that apply to the journal are still applicable. In no event shall the RSC be held responsible for any errors or omissions in these *Accepted Manuscript* manuscripts or any consequences arising from the use of any information contained in them.

View Online

Cite this: DOI: 10.1039/c0xx00000x

www.rsc.org/xxxxxx

ARTICLE TYPE

Dynamics of spontaneous emission of quantum dots in a one-dimensional cholesteric liquid crystal photonic cavity

Andrea L. Rodarte, Georgiy V. Shcherbatyuk, Laurel Shcherbatyuk, Linda S. Hirst* and Sayantani Ghosh*

Received (in XXX, XXX) Xth XXXXXXXXX 20XX, Accepted Xth XXXXXXXXX 20XX
DOI: 10.1039/b000000x

We investigate the modulation of recombination lifetimes of CdSe/ZnS quantum dots (QDs) dispersed in a cholesteric liquid crystal (CLC) photonic cavity. Using ultrafast spectroscopic techniques we focus on the time-resolved emission from QD ensembles in CLC matrices with either planar or homeotropic alignment. In the case of planar alignment and a well-defined spectral stop band (reflection band) we observe the emergence of a second, faster decay time less than 2 ns. This short recombination pathway is observed only in samples where the QD emission spectrum partially overlaps the CLC stop band by 50% or more. Samples prepared with homeotropic alignment do not have a stop-band, and consequently, do not lead to spectral or dynamical modulation of the QD emission. Our observations indicate that coupling between the excitonic and the photonic cavity modes results in an enhancement and modulation of spontaneous emission in the liquid crystal medium.

1 Introduction

Tailoring basic light-matter interactions for advanced applications is a major focus of researchers in photonics, semiconductor physics and materials science. Advances over the last decade in electron microscopy, sample fabrication, and synthesis have presented the means for manipulation and control of these interactions with remarkable precision down to micro and nano-scales. A typical example is the development of optical micro-resonators, with very high quality (Q) factors, which interact with light confined within their volumes to create lasing (1). Their size makes them attractive candidates for incorporation in on-chip devices that require small footprints and low threshold powers (2). These devices can be fabricated in a variety of geometries and one of these is the planar micro-cavity design based on the well-known photonic crystal template. This has the advantage of very small mode volume, resulting in ultra-high Q emission (3). Photonic band gap (PBG) cavities fabricated from semiconducting materials can support lasing emission of $Q > 10^5$ in the near infrared region (4). In spite of these attractive properties, PBG cavities are very fabrication intensive, and cannot be tuned easily *in situ*. An alternative approach to PBG cavities with micron scale active regions was developed in the last decade using liquid crystal (LC) materials (5) (6) (7). Certain chiral LC molecules self-assemble to form the cholesteric phase, characterized by a helical rotation of the director axis with a characteristic pitch (Fig. 1A, left inset) (8). This helical pitch results in a spectral stop-band (the reflection band) analogous to that seen in photonic crystals, and therefore cholesteric liquid crystal (CLC) materials can act as a fluid one-dimensional photonic cavity. CLCs have the advantage of not only being far easier to fabricate than their semiconducting counterparts, but their stop-bands can be spectrally tuned using either temperature or LC composition. Furthermore, the cavity effect can be reversibly switched on and off by an externally applied electric field. Dye-doped CLC films exhibit resonant emission at the long wavelength band-edge of the stop-band, which has led to the development of LC based dye lasers (9) (10) (11).

In this paper we investigate modulation of the dynamical spectral properties of chemically synthesized quantum dots (QDs) dispersed in CLC photonic cavities. QDs can be more suitable than organic dyes for certain applications, especially given the optical tunability offered by their size-dependent energy band-gaps and their higher photo-stability compared to most dyes (12). Further, they are isotropic emitters and therefore not subject to the polarization constraint that allows efficient amplification only at the long wavelength edge in anisotropic dyes (13) (14). The study of chemically synthesized QDs dispersed in LC materials is a relatively new research area. While it is expanding rapidly, prior work has been limited to nematic (15) and smectic (16) LC materials, where greater emphasis has been given to the effect of the QDs on the LC electro-optic properties. Most recently, we have demonstrated that in these systems QD emission is enhanced at both edges of the CLC stop-band, accompanied by a spectral red shift at the short wavelength edge of the stop-band and blue shift at the long edge. In addition, the resonant emission is elliptically polarized by the CLC cavity, with the ellipticity being a function of the emission wavelength (17). As a result, in a set-up such as a Cano-wedge cell (18), the polarization phase of the QD emission is both *spatially* and *spectrally* controllable. This last property is especially attractive. It not only opens up new possibilities to use these materials as novel opto-electronic and photonic components, but also has important implications for QD based quantum information processing schemes where precise modulation of emission frequency and phase is vital.

2 Experimental procedures

2.1 Sample preparation

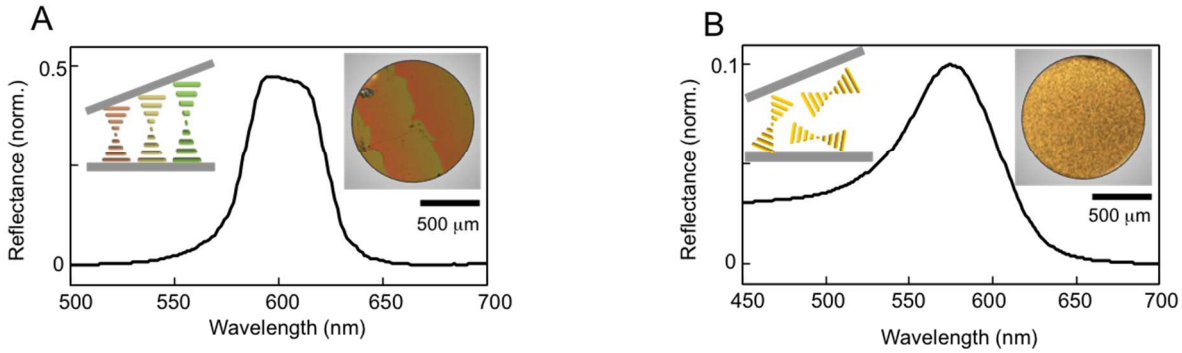

Figure 1 (A) Reflectance showing a well-defined stop-band in a CLC sample with planar alignment. Schematic (left inset) demonstrates the helical arrangement of the CLC in a Cano-wedge cell. The changing pitch creates the stripe pattern observed under POM (right inset). (B) Reflectance of a CLC sample with homeotropic alignment. Schematic (left inset) depicts random orientation of helices, which results in a homogenous transmission (right inset).

CLC samples were prepared by mixing cholesteryl oleyl carbonate (COC, Sigma Aldrich), and the nematic liquid crystal, 4'-pentyl'4-biphenylcarbonitrile (5CB, Sigma Aldrich). in varying proportions by weight. The LC mixtures are sonicated at 43°C (above the isotropic transition temperature for both compounds) for 1 hr to ensure good mixing. CdSe/ZnS QDs with octadecylamine ligands (NN Labs) and an emission in toluene solution centred at 609nm, are added to the LC mixtures at a concentration of 0.01-0.02 wt%, then sonicated again for 1-6 hrs to obtain the final QD-LC composite.

LC films were deposited between glass plates using two different alignment layers, planar (molecules lie parallel to the glass substrate) and homeotropic (molecules lie perpendicular to the substrate). To prepare a planar alignment coating, glass slides were spin coated with a 1% wt aqueous polyvinyl alcohol (PVA) solution (Sigma Aldrich), dried in air and rubbed to establish the required orientation. To prepare a homeotropic alignment layer, glass slides were dip coated for 5 minutes in 0.5 mM aqueous Hexadecyltrimethylammonium bromide (CTAB, Sigma Aldrich) solution. The isotropic liquid crystal mixture (at 40.0° C) was then pipetted onto the prepared glass slides, arranged to form a Cano-wedge cell, and then cooled at 0.1 °C/min to 30 °C to form the CLC phase using a Linkam STS350 hot-stage. Several different formulations were used in this study. Sample S1 contains 0.02 wt% QDs, dispersed in 59.6 wt % COC and 40.4 wt % 5CB. Samples S2, S3 and S4 contain 0.01 wt % QDs, dispersed in 59.4 wt % COC and 40.6 wt % 5CB. Sample S5 contains 0.01 wt % QDs dispersed in 59.1 wt % COC and 40.9 wt % 5CB. The control sample contains 0.01 wt % QDs dispersed in 74.8 wt % COC and 28.2 wt % 5CB. The purpose of varying the proportion of different LC compounds in the mix is to change the spectral position of the stop band. After cooling into the CLC phase, all samples were allowed to anneal for the same time prior to beginning measurements.

2.2 Measurement techniques

We verify the formation of the CLC phase in our samples using Polarized Optical Microscopy (POM). Fig. 1A (right inset) shows a transmission image of a QD-LC sample with planar alignment. The LC molecules are forced to align parallel to the glass slides, as shown in the schematic in Fig. 1A (left inset) but the increasing distance between the two slides forces the pitch to continuously elongate, which changes the spectral position of the stop-band, and hence, the colour of the CLC transmission. Once the distance between the glass plates is large enough to fit in another half-pitch, the colour gradient repeats itself, a pattern known as Grandjean steps. The stop-band of an arbitrary region of this sample is plotted in Fig. 1A, measured using a UV-VIS spectrophotometer. Fig. 1B shows the corresponding results for a homeotropicaly-aligned sample. The helices are now randomly oriented in a focal conic texture (Fig. 1B, left inset) and the transmission image in Fig. 1B (right inset) does not show the Grandjean steps. Initially after preparation, the homeotropic samples appear white in colour, implying wavelength independent scattering. However, as these samples anneal, a characteristic length scale forms, and as a result, the reflectivity (Fig. 1B, main) shows a much weaker, broad peak instead of a well-defined stop-band.

Further spectral characterization is done using a custom-designed scanning photoluminescence (PL) confocal microscopy system. The excitation source used is a 532 nm continuous wave laser focused on the sample through a high NA objective to produce a diffraction-limited spot size (~ 600 nm). The samples are mounted on a heat controlled motorized 3D scanning stage with lateral resolution of 40 nm. The PL from the QDs is collected by the same objective and dispersed by an Acton 300i spectrometer onto a thermoelectrically cooled CCD (spectral resolution ~ 0.18 nm). Using this arrangement, we raster scan selected regions of the sample to create spatially resolved PL maps. For the time-resolved measurements we use an ultrafast Ti:Sapphire with 76 MHz repetition rate and pulse width of 150 fs as our excitation source. The laser output is frequency doubled to produce an excitation wavelength of 400 nm with the final power reduced to 7 μW. The spectrometer is coupled to a single photon avalanche detector with a time-correlated single photon counting system (PicoHarp 300) with an instrument response function of 12 ps.

3 Results and Discussions

In Fig. 2 we show spatially-resolved maps of the peak QD emission wavelength (λ_{PEAK}) for sample S1. Figs. 2A and 2B correspond to the planar aligned sample when the emission is polarization-resolved at 0° and 90° to the rubbing direction (black arrow) from the same region. The dotted line in Fig. 2A highlights the QD emission red-shifting across a Grandjean step. It has been recently shown (17) that this effect results from a coupling between QD emission and the cholesteric stop band. When viewed from an orthogonal polarization, the λ_{PEAK} blue-shifts across the same step in Fig. 2B. This complimentary pattern can be explained by the elliptical polarization of the QD-cavity coupled emission (17) (19). The ellipticity is both wavelength and position dependent and is therefore dominated by the short (long) emission wavelength in the case of parallel (perpendicular) polarization set up at the start of each step. Figures 2C and 2D are similar PL scans of the same area in a QD-LC sample with homeotropic alignment, taken along one spatial axis (which we

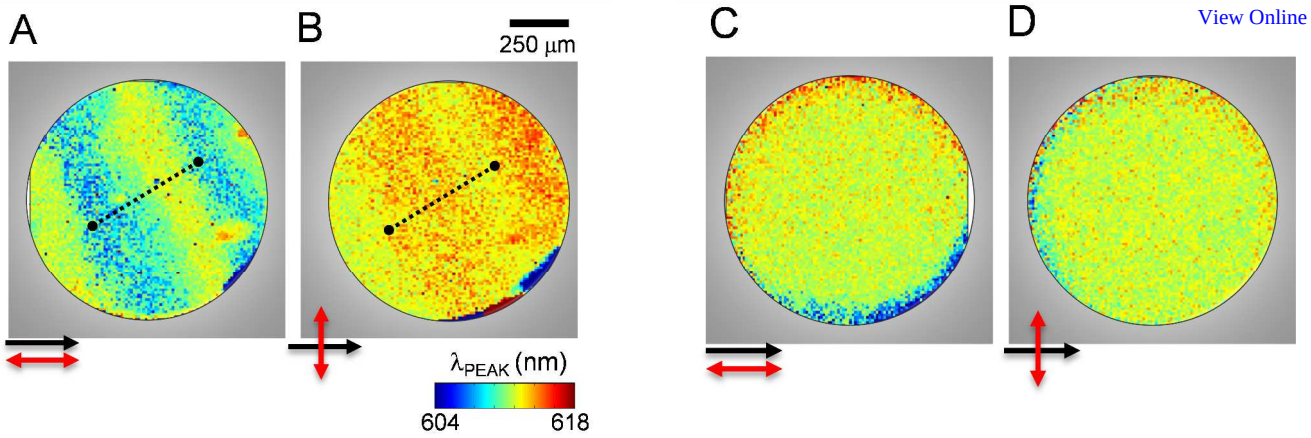

Figure 2 Scanning PL images of QD-CLC sample S1. Spatially-resolved QD peak emission wavelength is plotted for planar alignment with collection polarization direction (A) parallel and (B) perpendicular to the rubbing direction. Images show complementary color change across a step along the dotted lines. Similar scans for homeotropic alignment with (C) parallel and (D) perpendicular polarization configurations showing homogenous and polarization-independent QD emission.

designate 0°) and then along another after a 90° sample rotation. As expected, without the presence of a well-defined stop-band and resulting Grandjean steps, the QD emission is uniform and polarization-independent.

Spectral modulations of QD emission as observed in Fig. 2 are often accompanied by changes in the recombination rate. When suspended in solution, chemically-synthesized QDs have a recombination process described by an exponential decay with a single time-scale $I(t) = Aexp(-t/\tau_S)$ and the recombination rate, which is wavelength independent, is given by $K_S = 1/\tau_S$. For the QDs used in our samples the recombination lifetime (in solution) $\tau_S \sim 13$ ns. (20).

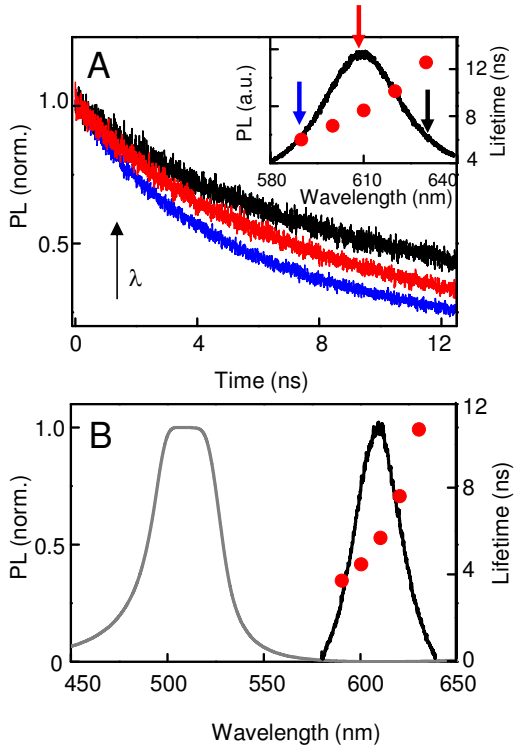

Figure 3 (A) Spectrally-resolved, time-resolved PL taken at three points along the QD emission spectrum (indicated by arrows in the inset) for control sample at 43 °C. Recombination times obtained from exponential fits are plotted in the inset and show QD lifetime increasing with wavelength as a consequence of inter-QD resonant energy transfer. (B) CLC stop-band and QD emission spectrum for the control sample at 25 °C. QD recombination decay shows one characteristic lifetime (solid circles).

We begin our investigation of QD recombination lifetimes in the CLC photonic cavity with a control sample where the CLC stop-band does not overlap with the QD emission spectrum. Fig. 3A (inset) shows the QD emission spectrum at 43°C when the CLC is in the isotropic phase. The arrows indicate the points along the spectrum where time-resolved data is presented in the main part of Fig. 3A. The normalized curves for 590, 610 and 630 nm show that the recombination lifetime is now wavelength dependent and increases monotonically with emission wavelength (inset, solid circles). This variation is most likely not a result of dispersion in the CLC, as it is typically observed in any ensemble where the QDs are not isolated, but have dipole-dipole inter-particle interactions that allow non-radiative energy transfer from the smaller QDs to the larger ones. This energy transfer introduces an additional relaxation channel for the smaller QDs, increasing their total recombination rate (21). We can estimate the efficiency of this energy transfer as $\varepsilon = 1 - (\tau_\lambda/\tau_S)$ where τ_λ is the recombination lifetime in the CLC sample at a particular wavelength and τ_S is the lifetime in solution (22). This gives us an ε of 62% at 590 nm which decreases to 38% at 610 nm, and by 630 nm is a very small 6%. In comparison, a close-packed film of these QDs would have almost 90% efficiency at the lowest wavelengths (23). Since dipole-dipole interactions fall off as ~ $1/r^3$, the comparative smaller ε values in the QD-CLC samples are not surprising. Fig. 3B shows spectra and recombination lifetimes when the control sample is cooled to 25°C. The CLC has a distinct stop-band that has no overlap with the QD spectrum. As a result, the recombination process is relatively unperturbed and follows a single exponential decay. Across the spectral range of the emission curve, the lifetime τ varies from 4 – 11 ns (solid circles), similar to that observed in the isotropic phase.

As in the case of the dipole-dipole coupling between QDs, coupling between the photon of an emitter and the resonance mode of the cavity it is embedded in also causes faster decay of spontaneous emission, a phenomenon known as the Purcell effect (24) (25) (26). Given that QD emission is amplified in the cholesteric phase due to photonic confinement, it is possible that recombination dynamics would be modulated as well. In Fig. 4A we plot the CLC stop-band and the QD emission spectra for sample S2, and superimposed on these are the recombination lifetimes extracted from the corresponding spectrally-resolved, time-resolved PL curves. In the spectral region where the normalized QD emission has 50% or more overlap with the stop-

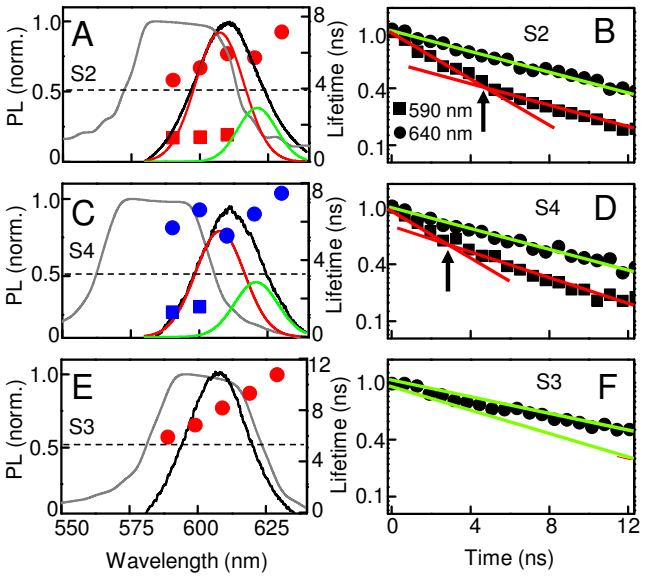

Figure 4 Recombination times for QD-CLC samples S2, S4 and S3, (planar alignment) superimposed on QD emission spectra and the CLC stop-bands. (A, C) QD emission in samples S2 and S4 have partial overlap with CLC stop-band and can be resolved in to two curves. Time-resolved QD PL demonstrates two characteristic lifetimes (solid circles and squares) for the wavelength range that has substantial spectral overlap with the stop band. (B, D) Corresponding time-resolved data at 590 and 640 nm plotted on a semi-log scale. Linear fits show the presence of two lifetimes at 590 nm and one lifetime at 640 nm. (E) Sample S3, where the QD emission has complete overlap with the stop-band and exhibits a single recombination time (solid circles) across all wavelengths. (F) Corresponding time-resolved data at 590 and 640 nm.

band, the QD PL has two characteristic lifetimes. The longer of the two, τ_1 (circles), is consistently shorter than the single recombination lifetime observed in the control sample, although it increases with emission wavelength as well. Further, it is now accompanied by a faster lifetime, τ_2 (squares), less than 2 ns. The recombination process can now be described by the function, $I(t) = A_1 exp(-t/\tau_1) + A_2 exp(-t/\tau_2)$, with a total recombination rate equal to $K = 1/\tau_1 + 1/\tau_2$. We note that the spectral region outside the stop-band still has a single decay rate. Fig. 4B shows the time-resolved data from the two extremes of the emission spectra, at 590 nm and 640 nm, on a semi-log scale. The recombination curve at 590 nm clearly has two distinct slopes, signifying the two lifetimes, while the curve at 640 nm has a single lifetime. Figs. 4C and 4D show similar data from sample S4, and we again observe two recombination lifetimes in the spectral region where there is partial overlap between the stop-band and QD emission spectra.

To correlate the lifetime changes to cavity effects further, we examine samples where the CLC cavity modes and alignment are different from those studied above. Fig. 4E shows results from sample S3 where the QD emission spectrum lies entirely within the stop-band. In this case there is suppression of the entire QD emission by the photonic cavity indicating no QD-cavity coupling. The time-resolved data is now characterized by a single exponential decay over the entire QD emission spectral range, as seen in Fig. 4F. Further, the decay times in these QDs are consistently longer than the long lifetime τ_1 in the other two samples where the cavity modulates the QD emission. In this sample at the longest emission wavelength the recombination time is almost equal to the average isolated QD lifetime observed in solution and similar to that observed in the control sample (Fig. 3B). In Fig. 5 we compare results from the planar and homeotropic versions of sample S5. The planar sample has a

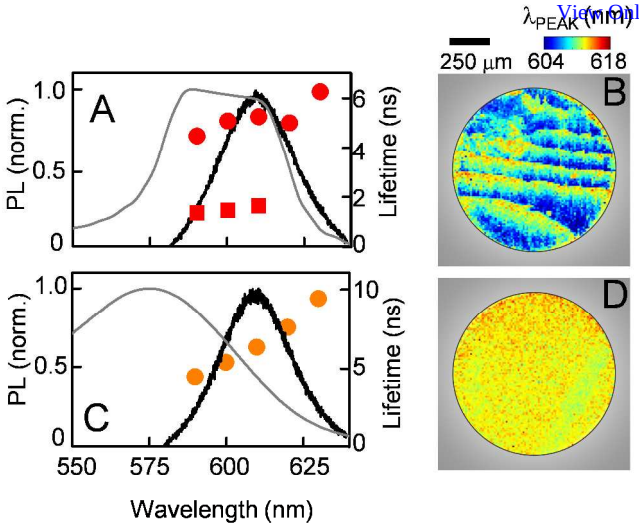

Figure 5 Comparison of recombination times in sample S5 with (A) planar and (C) homeotropic alignment. Corresponding spatially-resolved PL maps of peak emission wavelengths are shown in (B) and (D).

well-defined stop-band where the long edge overlaps with the QD spectrum. As a result, we observe the stripe pattern in the spatially-resolved PL map (Fig. 5B) signifying the expected QD spectral modulation, as well as a second decay time in the wavelength range that lies within the stop-band (Fig. 5A, solid circles). In comparison, the homeotropic sample does not exhibit a clear reflection band and shows a broad peak much lower in absolute intensity (Fig. 5C) and while that peak does overlap with the QD emission, it does not result in either the stripe formation (Fig. 5D) in λ_{PEAK} or in introducing a second recombination pathway. As expected, the time-resolved data shows a single lifetime similar to Fig. 3B.

Data shown in Figs. 4E – F and 5A – B lead us to conclude that the alteration of recombination dynamics is not due solely to the emission suppression inside the stop-band, nor due to the presence of the CLC medium. The second, faster lifetime observed in Figs. 4A – D appear only in samples where two conditions are simultaneously satisfied. First, the CLC forms a photonic cavity with a well-defined spectral stop-band, and second, the QD spectrum has partial overlap with the stop-band to allow band-edge amplification. Analysis of the QD emission in Figs. 4A and 4C show that while the QD spectra in the isotropic phase can be fitted by a single curve, each spectrum in the CLC phase is actually a superposition of two emission spectra. These fits, shown in Figs. 4A and 4C, suggest these are contributions from two subsets of QDs, ones that emit inside, and ones outside the stop band. Emission from the former subset is amplified and these constitute the 'resonant' modes that dominate the total emission. The other subset is the collection of the 'non-resonant' modes. The cavity coupling enhances the spontaneous recombination rate, associated with the Purcell effect, only in the QDs that emit in the resonant modes while the non-resonant modes are left unaltered.

Conclusions

Photonic cavities based on LC materials are attractive because their optical characteristics are easily tunable. For example, the spectral position of the stop band can be altered by varying the proportion of different LC compounds in the mix, or, the cavity effects can be switched on-off by using temperature to change the LC phase or electric fields to disrupt the cholesteric texture.

These properties have been exploited to design LC based dye lasers. Unlike these dyes, QDs are quantum systems that possess unique functionalities that allow them to function as ideal qubits in quantum information processing devices. The ability to control QD properties is therefore an important capability, and we have shown that these CLC cavities can control both the phase and the peak emission wavelengths of an ensemble of embedded QDs. In addition, here we have demonstrated dynamical modulation of the QD spontaneous emission by the CLC photonic cavities, with Purcell factors between 3.8 – 4.2 for our samples (see Electronic Supplementary Information), when expressed as the ratios of recombination times with and without cavity coupling. This rate increase is spectrally-selective, as it is only observed for the subset of QDs that emit resonantly with the stop-band. This dynamic control can lead to the development of QD based opto-electronic devices, such as single photon sources. Given the additional functionalities that the liquid crystal matrices can provide, the systems we have investigated can form the basis of other new applications, such as faster, interactive displays, and tunable and flexible components for 4th generation photovoltaics.

Notes and references

The authors acknowledge funding from UC SOLAR and UC MERI.

Department of Physics, University of California, Merced, Ca 95343, USA. E-mail: lhirst@ucmerced.edu, sghosh@ucmerced.edu

1 T. J. Kippenberg, R. Holzwarth and S. A. Diddams, *Science,* 2011, **332**, 555.
2 D. K. Armani, T. J. Kippenberg, S. M. Spillane and K. J. Vahala, *Nature,* 2003, **421**(27), 925.
3 S. Tomljenovic-Hanic, A. D. Greentree, C. Martijn de Sterke and S. Prawer, *Optics Express,* 2009, **17**(8) 6465.
4 Y. Zhang and M. Loncar, *Optics Express,* 2008, **16**(22), 17400.
5 M. Mitov, E. Nouvet and N. Dessaud, *The European Physical Journal E,* 2004, **15**, 413.
6 S. S. Choi, S. M. Morris, W. T. S. Huck and H. J. Coles, *Advanced Materials,* 2009, **21**(38-39), 3915.
7 J.-C. Yang, C.-S. Kee, J.-e. Kim and H. Y. Park, *Physical Review E,* 1999, **60**, 6852.
8 P. J. Collings, Liquid Crystals: *Nature's Delicate Phase of Matter, Princeton*, NJ: Princeton University Press, 2002.
9 S. Furumi, S. Yokoyama, A. Otomo and S. Mashiko, *Applied Physics Letters,* 2003, **82**(1), 16.
10 V. I. Kopp, Z.-Q. Zhang and A. Z. Genack, *Progress in Quantum Electronics,* 2003, **27**, 369.
11 V. I. Kopp, B. Fan, H. K. M. Vithana and A. Z. Genack, *Optics Letters,* 1998, **23**(21), 1707.
12 U. Resch-Genger, M. Grabolle, S. Cavaliere-Jaricot, R. Nitschke and T. Nann, *Nature Methods,* 2008, **5**, 763.
13 J. Schmidtke and W. Stille, *The European Physical Journal B,* 2003, **31**, 179.
14 B. Taheri, A. F. Munoz, P. Palffy-muhoray and R. Twieg, *Molecular Crystals and Liquid Crystals,* 2001, **358**, 73.
15 B. Kinkead and T. Hegmann, *J. Mater. Chem.*, 2010, **20**, 448.
16 G. A. Shandryuk, E. V. Matukhina, R. B. Vasil'ev, A. Rebrov, G. N. Bondarenko, A. S. Merekalov, A. M. Gas'kov and R. V. Talroze, *Macromolecules*, 2008, **41**, 2178.
17 A. L. Rodarte, C. Gray, L. S. Hirst and S. Ghosh, *Physical Review B,* 2012, **85**, 035430.
18 P. G. de Gennes and J. Prost, *The Physics of Liquid Crystals 2nd ed.*, Oxford: Clarendon, 1993.
19 A. L. Rodarte, C. G. L. Ferri, C. Grey, L. S. Hirst and S. Ghosh, *Proc. of SPIE,* 2012, **8279**, 82790H.
20 G. V. Shcherbatyuk, R. H. Inman and S. Ghosh, *Journal of Applied Physics,* 2011, **110**, 053518.
21 S. A. Crooker, J. A. Hollingsworth, S. Tretiak and V. I. Kimov, *Physical Review Letters,* 2002, **89**(18), 28.
22 J. R. Lakowicz, *Principles of Fluorescence Spectroscopy, 2nd ed.*, New York: Kluwer Academic, 1999.
23 G. V. Shcherbatyuk, P. Talbot and S. Ghosh, *Applied Physics Letters*, 2012, **100**, 212114.
24 J.-Y. Zhang, X.-Y. Wang and M. Ziao, *Optics Letters,* 2003, **28**(16), 1430.
25 B. Gayral, J.-M. Gerard, B. Sermage, A. Lemaitre and C. Dupuis, *Applied Physics Letters,* 2001, **78**(19), 2828.
26 H. Lohmeyer, C. Kruse, K. Sebald, J. Gutowski and D. Hommel, *Applied Physics Letters,* 2006, **89**, 091107.